LIGHT INDUCED DEGRADATION IN PROMISING MULTI-CRYSTALLINE SILICON MATERIALS FOR SOLAR CELL FABRICATION

B. Damiani[1], K. Nakayashiki[1], D. S. Kim[1], V. Yelundur[1], S. Ostapenko[2], I. Tarasov[2] and A. Rohatgi[1]
1. Georgia Institute of Technology, Atlanta, GA 30332-0250
University Center of Excellence for Photovoltaics (UCEP)
2. University of South Florida, Tampa, FL 33620
Nanomaterials and Nanomanufacturing Research Center (NNRC)

ABSTRACT

Light induced degradation (LID) in boron doped Czochralski (Cz) silicon with high oxygen content is known to degrade solar cell efficiency. Multicrystalline Si crystals also have oxygen and use B doping, but LID effects are largely unknown. In this paper, ribbon, Cz, and cast multi-crystalline Si crystals with a resistivity of 1-3 Ωcm were investigated for LID. 15-16% efficient EFG, String Ribbon, and cast mc-Si solar cells, fabricated by manufacturable screen printed technology, show small but measurable LID (0.2% absolute efficiency loss). In less than 15% efficient devices, LID was not detectable in ribbon Si crystals. However, >16% efficient photo-lithography ribbon Si degraded >0.5% absolute. Analysis of the bulk lifetime using photoluminescence mapping, after cell processing, supports the presence of LID in the good regions of the ribbon materials while the defective regions remained essentially unaffected.

INTRODUCTION

Boron doped Czochralski (Cz) silicon with high oxygen content is known suffer LID, decreasing the stabilized solar cell efficiency [1]. This results from a decrease in the minority carrier lifetime after exposure to carrier injection. The LID-induced loss in efficiency for screen-printed Cz Si cells can lead to a 10% drop in relative efficiency or >1.5% absolute. In order to decrease the cost of solar cells for manufacturing, many different silicon crystal growth techniques are being explored. All the materials currently use boron as the bulk dopant and incorporate various levels of oxygen. A linear relationship between the substitutional Boron (B_s) concentration and LID trap formation has been reported by various researchers [2]. The relationship to interstitial oxygen (O_i) concentration has not been so straightforward. As high as a fifth order relationship and as low as a first order relationship has been proposed [3]. The most recent proposal is a quadratic relationship with the fast diffusing oxygen dimmer (O_{2i}) [3]. The extent or existence of LID on lower cost mc-Si is largely unknown. In these materials, the as grown lifetimes are in the range of 1-10 µs and are dominated by other impurities and defects. LID has been observed in Cz and some cast mc-Si with greater than 5-10 µs minority carrier lifetime [4]. For example, in order to observe LID in cast mc-Si a phosphorus gettering step is employed to increase the bulk lifetime so LID data is not obscured. De Wolf et al. demonstrated LID in very low resistivity (<0.2 Ωcm) cast mc-Si as a function of wafer position in an ingot [4]. Oxygen content was shown to increase from undetectable (25°C) for the top of the ingot to 4×10^{17} cm^{-3} near the bottom of the ingot. Solar cells fabricated from the top of the ingot showed little efficiency degradation while cells from the bottom showed increased LID despite the decreasing B doping concentration with ingot depth that would act to decrease LID.

This paper reports on the degree of solar cell efficiency degradation resulting from LID in some of the promising materials for industrial manufacturing of solar cells. String Ribbon (SR) from Evergreen, Edge Defined Film Feed Growth (EFG) ribbon, cast mc-Si grown by the Heat Exchanger Method (HEM), B doped Cz, Ga doped Cz, and B doped web Si from Ebara were analyzed. In selected cases cells with photolithography contacts were also made.

EXPERIMENTAL

In order to check for the characteristic degradation / recovery cycle due to LID effect in the promising silicon materials, first phosphorus gettering with in-situ oxidation for passivation was performed on Si wafers. Subsequently SiN_x was deposited on both sides of the wafer for enhanced passivation. Lifetime measurements were made using the quasi-steady state photoconductance (QSSPCD) lifetime measurement technique. Additional samples were prepared for lifetime measurement by etching the solar cell down to bare Si and coating it with a SiN_x layer for surface passivation on both sides. Solar cell efficiencies were measured under AM 1.5 global conditions after various exposure to illumination and annealing to check for degradation and annealing. Oxygen data was obtained by Fourier Transform Infra-Red (FTIR) spectroscopy, using a Digilab FTS40-pro. Scanning room-temperature photoluminescence was applied for lifetime mapping of wafers with and without LID, using a novel photoluminescence scanning setup (SPEX-500M) [5].

RESULTS

Initial measurements were made on phosphorus gettered mc-Si samples. Figure 1 shows the area averaged lifetime data obtained via QSSPCD for the ribbon and cast mc-Si materials at 5×10^{14} cm^{-3} injection level. After phosphorus gettering step, different materials had different lifetimes ranging from 3-30 µs. Cast mc-Si, EFG, and web showed detectable degradation / recovery. Only the SR sample did not show LID, probably because the very low lifetime, due to the absence of defect hydrogenation, acted to obscure the LID.

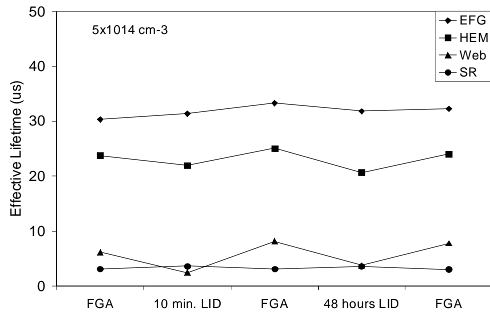

Fig. 1 QSSPCD effective lifetime data for ribbon and cast mc-Si

Figure 2 shows the efficiency dependence on LID for manufacturable screen-printed (SP) solar cells on these materials. Initial efficiencies for all materials (except web, where the ~100 μm thickness and somewhat lower efficiency obscures degradation) was over 15%. Along with the B doped Cz (0.8 Ωcm) solar cell, the HEM (1.5 Ωcm) , EFG (~3 Ωcm), and SR (~3 Ωcm) solar cells also degrade but not as much (see Fig. 2), partly due to the lower base resistivity of the substrates. The Cz sample

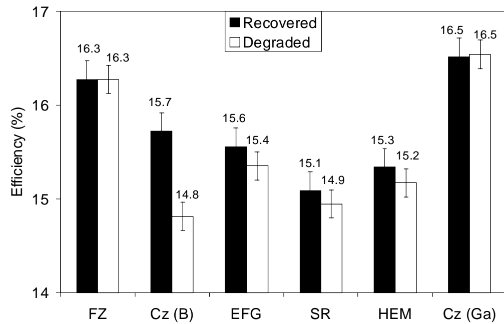

Fig. 2 Average efficiency change after 4 degradation / recovery cycles for mc-Si solar cells

showed a ~1% drop in absolute efficiency compared with only 0.2% absolute for the other materials. The ribbon material, after the phosphorus gettering, did not show significant degradation (see Fig. 1). The bulk lifetime in the finished devices is much higher than the as-grown or even phosphorus gettered samples due to hydrogenation [6]. Table I shows the most recent data available to our knowledge on interstitial oxygen (O_i) content in these promising crystalline Si materials.

Table I. Current O_i concentration in promising crystalline Si materials [9-11].

Interstitial Oxygen Concentration (O_i) cm^{-3}				
FZ	$<10^{15}$		Web	10^{18}
SR	$4\text{-}8x10^{16}$		(B) Cz	$\sim10^{18}$
EFG	$<5x10^{16}$		(B) MCz	$10^{16}\text{-}5x10^{17}$
HEM	$<4x10^{-17}$		(Ga) Cz	$\sim10^{18}$

It is important to note that there is small variation in oxygen content of the ribbon materials. The oxygen concentration has varied over the years as the ribbon growth techniques evolved. It is possible that oxygen concentration now maybe different than reported in this table. In the case of cast mc-Si ingot, the O_i concentration is dependent on position within the ingot. Therefore, in this study, thick mc-Si wafers were obtained to determine the oxygen concentration by FTIR as a function of ingot position. Figure 3 shows the room temperature FTIR spectroscopy data for the oxygen interstitial peak in a directionally solidified HEM ingot as a function of position. The oxygen concentration increased from top to bottom with a quenching of oxygen at the very bottom. Despite the varying O_i content and base doping level the ribbon and cast mc-Si screen printed (SP) samples showed similar degradation (0.2%) for ~15% SP cells. In order to

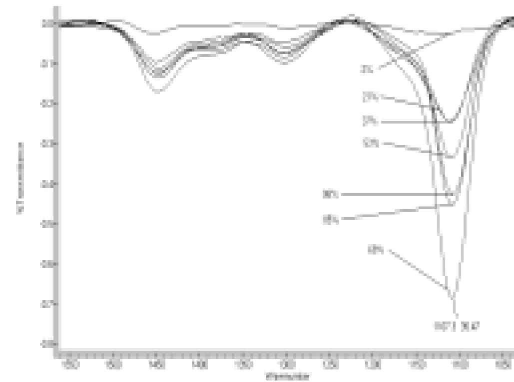

Fig. 3 Room-temperature FTIR spectra show O_i concentration in HEM mc-Si as a function of wafer position from the top of the ingot (0%) to the bottom of the ingot (100%). Undetected - $4x10^{17}$

understand the reason for this, we investigated the post processing lifetime in the ribbon materials and performed spatially resolved photoluminescence measurements. Figure 4 shows the characteristic degradation curve of the minority carrier lifetime in a EFG sample after solar cell fabrication, including hydrogenation. The sample showed a drop in lifetime down to 22 μs at $5x10^{14}$ cm^{-3} injection level. The recovered lifetime at $5x10^{14}$ cm^{-3} was ~30 μs. Ribbon materials are known to benefit greatly from processing with hydrogenation, which may increase the

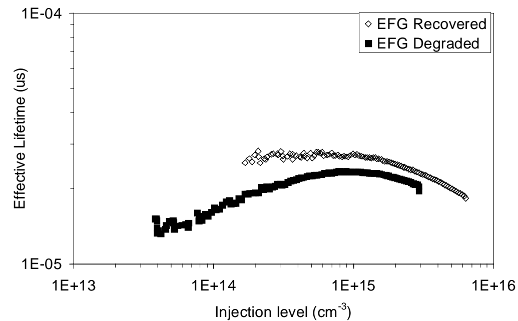

Fig. 4 Effective lifetime verses injection level for processed hydrogenated solar cell

overall lifetime from ~1-5µs to over 30µs [6].

Additional samples were examined to understand and quantify the LID effect in very good and average cells. Table II shows the change in important solar cell parameters for these materials. Preliminary investigations of LID in a very high efficiency SR (>17%) and EFG (~16%) samples with photolithography front contacts (initial V_{oc}= 619 and 612 mV respectively) showed a higher (0.5% and 0.9%) efficiency degradation compared to the >15% SP cells (see Fig. 2). Further investigation is required to determine if this was the result of higher than normal oxygen in these ribbon samples or higher starting efficiency and other factors. Additionally, screen printed SR and EFG cells with efficiencies in the range of ~13.5-15% showed negligible degradation because the lower lifetime obscures the LID.

Table II. Efficiency degradation after 3 days illumination of ~0.5 suns for various efficiency mc-Si wafers.

mc-Si type	ΔV_{oc} (mV)	ΔJ_{sc} (mA/cm^2)	ΔEff. (%)
SR 17.1%	9.1	0.44	0.50
SR 13.3%	0.0	0.0	0.00
EFG 16.0%	19.0	0.93	0.90
EFG 14-15%	0.0	0.01	0.03
HEM 15.6%	4.0	0.47	0.28
HEM 15.3%	2.0	0.13	0.04

Interestingly, the HEM samples with comparable efficiencies show varying efficiency degradation (0.3% and 0.04%). This is possibly due to difference in O_i content of these wafers, as shown in Fig. 3 and [4]. Thus more accurate knowledge of O_i is needed to properly explain the variation in the LID behavior observed in these materials.

In order to improve the understanding of the effect of LID in the ribbon materials, a spatially resolved PL mapping technique was applied. This technique gives a map of the band to band PL maximum intensity at the energy of 1.09eV and independently the intensity map of a "defect" PL band with maximum at ~0.8eV. Using I_{bb} values it is possible to quantify the minority carrier lifetime through the following relationship [5] :

$$I_{bb} \sim \frac{\tau_{rad}^{-1}}{\left(\tau_{rad}^{-1} + \tau_{nr}^{-1}\right)} \qquad (1)$$

where I_{bb} is the intensity of the band to band recombination, and τ_{rad} and τ_{nr} are the radiative band-to-band lifetime and non-radiative lifetime respectively. The non-radiative lifetime is dominant in silicon at room temperature and is proportional to the effective lifetime (τ_{eff}). The τ_{rad} is a material constant and much larger than the τ_{nr} therefore:

$$I_{bb} \sim \tau_{nr} / \tau_{rad} \sim \tau_{eff} / \tau_{rad} \sim \tau_{eff} \qquad (2)$$

which enables the same analysis of the LID trap (N_{LID}^*) used in photoconductance lifetime measurements [3]:

$$N_{LID}^* = I_{bb}(\deg)^{-1} - I_{bb}(rec)^{-1} \qquad (3)$$

where N_{LID}^* is the effective normalized trap concentration determined from the change in band to band PL intensity, I_{bb}(deg) is band to band intensity of a Si wafer in a degraded state and I_{bb}(rec) is the intensity in the recovered state. Figure 5 shows two PL maps of a B doped Cz-Si wafer degraded and recovered. The PL map shows a uniform distribution of the intensity (~N_{LID}^*) across the entire wafer in the degraded state as well as the recovered state. PL maps were also obtained for ribbon Si wafers passivated with SiN_x on top and bottom surfaces. Analogous to the band to band recombination in Si, we observe a defect band associated with areas of reduced

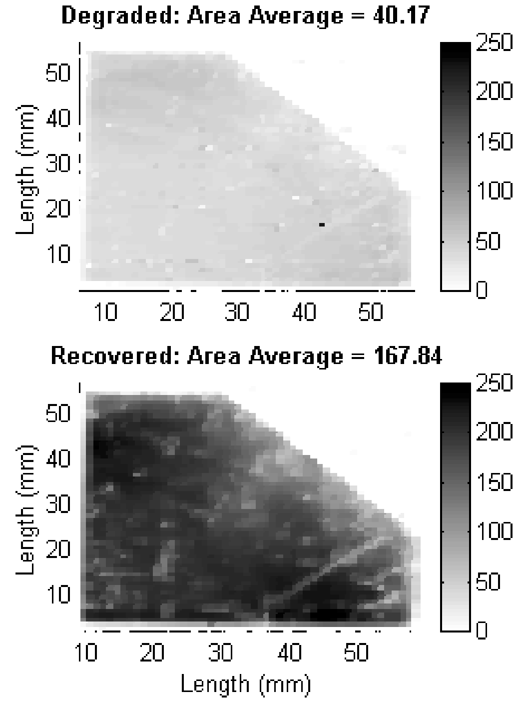

Fig. 5 PL map of a quarter B doped Cz Si wafer before and after LID.

lifetime, which is typical for ribbon materials [5]. Radiative recombination in defective materials give rise to a ~0.8 eV spectra. Ribbon materials often have this quality and therefore can provide additional information. In Figure 6, a line scan of lifetime area map of a EFG wafer before and after degradation of the I_{bb} as well as the defect band I_{db} is shown. Note that the LID degradation / recovery cycle is limited to the band to band spectra and occurs at different magnitudes according to crystal location. LID was observed away from low intensity (low lifetime) defect regions. Strong LID was observed in the high PL intensity regions. The sharp drop in the spectral intensity corresponds to defect locations and causes the LID data to be obscured (or at least more noisy). The I_{db} line scan shows the excellent spatial resolution in PL mapping. The mean values of the N_{LID}^* across the whole

Cz-Si and EFG wafers were 0.019 and 0.0061, respectively. No additional peaks were observed in the full PL spectrum for the degraded samples. Therefore the LID trap is not a radiative trap with > 0.8 eV energy, further supporting a near midgap trap location. This also helps to explain the lack of efficiency degradation observed in lower efficiency (or low lifetime) ribbon solar cells that are dominated by defective regions.

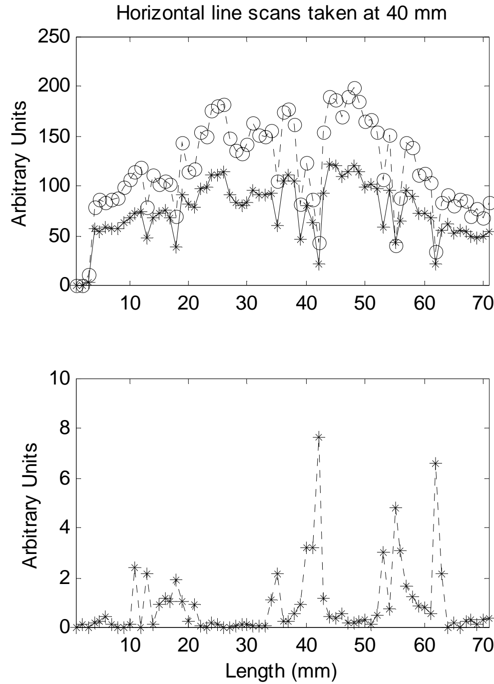

Fig. 6 Line scans of EFG (after solar cell processing) before and after LID of the I_{bb} and I_{db}

In an effort to gain a better understanding of the trap behavior using the PL mapping technique, a partial shading experiment was used to block light from being incident on a portion of a B doped Cz wafer. A 3 cm thick aluminum block was used to shade a low intensity light for 60 minutes. Figure 7 shows the resultant PL map. The area exposed to the low intensity room light showed degradation, while the covered portion of the wafer maintained a much higher lifetime. This was simultaneously confirmed using a surface photo-voltage diffusion length measurement. The area of interest is the boundary between the shaded and exposed region. By spatially confining the injected carrier concentration careful analysis of the transition region between the degraded section and the shaded section should result in trap diffusivity information.

CONCLUSIONS

Boron doped Cz Si (~300 μm) showed significant LID, resulting in 1-1.5% degradation in absolute efficiency. Ribbon Si materials are found to exhibit LID. The LID effect was smaller in SP mc-Si materials due to slightly higher resistivities for ribbon crystals, lower oxygen concentrations, and higher densities of defective regions. Cast mc-Si is shown to degrade 0.2-0.3% in some cases but not in the others (0.04%), depending on the position of the wafer in the ingot. This is partly attributed to the variation in oxygen content in the ingot. The top of the ingot has undetectable O_i but the bottom section can contain $4x10^{17}$ cm^{-3}. Photoluminescence maps were taken to provide a spatially resolved picture of the behavior of the trap responsible for LID. Strong LID was observed away from defect regions in EFG Si.

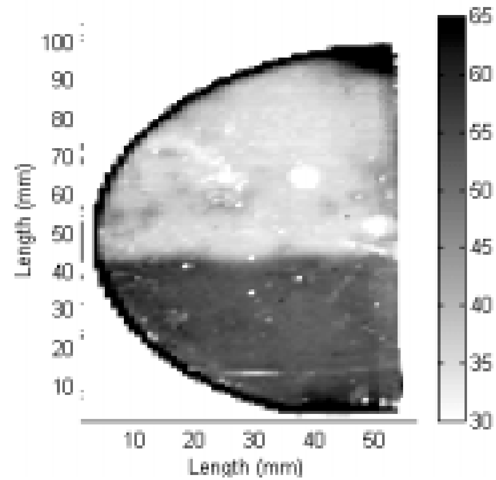

Fig. 7 PL map of a half wafer of B doped Cz Si subjected to shading by a aluminum block on the bottom ~42-43 mm.

REFERENCES

[1] J. Schmidt, A.G. Aberle, and R. Hezel, "Investigation of Carrier Lifetime Instabilities in Cz-Grown Silicon", *Proceedings of the 26th IEEE PVSC*, p.13 (1997)

[2] S. Glunz, S. Rein, J. Lee, and W. Warta, "Minority Carrier Lifetime Degradation in Boron-Doped Czochralski Silicon", *J. Appl. Phys.*, **90**, 2397 (2001)

[3] J. Schmidt, K. Bothe, and R. Hezel , "Formation and Annihilation of the Metastable Defect in Boron Doped Czochralski Si", *Proceedings of the 29th IEEE PVSC.*, p.432, (2002)

[4] S. De Wolf, P. Choulat, et al., "Light-Induced Degradation of Very Low Resistivity Multi-Crystalline Silicon Solar Cells, *Proceedings of the 28th IEEE PVSC,* p.53 (2000)

[5] S. Ostapenko, I. Tarasov, J. P. Kalejs, et.al "Defect Monitoring Using Scanning PL Spectroscopy in mc-Si Wafers", Semicond. Sci. Technol. **15**, 840 (2000)

[6] J. Jeong, Y. Cho, A. Rohatgi, et al.,"Rapid Thermal Processing for PECVD SiN-Induced Hydrogenation of High-Efficiency EFG Silicon Solar Cells", *Proceedings of the 29th IEEE PVSC*, 250 (2002)

[7] Private discussion with Evergreen

[8] J. Kalejs, "Silicon Ribbons and Foils-State of the Art" , *Solar Energy Mat. & Solar Cells*, **72**, p.139 (2002)